Available online at www.sciencedirect.com
ScienceDirect
Bioorganic & Medicinal Chemistry Letters 17 (2007) 602–608
Bioorganic & Medicinal Chemistry Letters

Discovery of [7-(2,6-dichlorophenyl)-5-methylbenzo [1,2,4]triazin-3-yl]-[4-(2-pyrrolidin-1-ylethoxy)phenyl]-amine—a potent, orally active Src kinase inhibitor with anti-tumor activity in preclinical assays

Glenn Noronha,[a,*] Kathy Barrett,[a] Antonio Boccia,[a] Tessa Brodhag,[a] Jianguo Cao,[a] Chun P. Chow,[a] Elena Dneprovskaia,[a] John Doukas,[a] Richard Fine,[b] Xianchang Gong,[a] Colleen Gritzen,[a] Hong Gu,[c] Ehab Hanna,[a] John D. Hood,[a] Steven Hu,[a] Xinshan Kang,[b] Jann Key,[a] Boris Klebansky,[b] Ahmed Kousba,[a] Ge Li,[c] Dan Lohse,[a] Chi Ching Mak,[a] Andrew McPherson,[a] Moorthy S. S. Palanki,[a] Ved P. Pathak,[a] Joel Renick,[a] Feng Shi,[c] Richard Soll,[a] Ute Splittgerber,[a] Silva Stoughton,[a] Suhan Tang,[c] Shiyin Yee,[a] Binqi Zeng,[a] Ningning Zhao[a] and Hong Zhu[a]

[a]*TargeGen, Inc., 9380 Judicial Drive, San Diego, CA 92121, USA*
[b]*BioPredict, Inc., 660 Kinderkamack Road, Oradell, NJ 07649, USA*
[c]*WuXi PharmaTech Ltd, Shanghai, PR China*

Received 26 September 2006; revised 1 November 2006; accepted 2 November 2006
Available online 7 November 2006

Abstract—We describe the identification of [7-(2,6-dichlorophenyl)-5-methylbenzo [1,2,4]triazin-3-yl]-[4-(2-pyrrolidin-1-ylethoxy)phenyl]amine (**3**), a potent, orally active Src inhibitor with desirable PK properties, demonstrated activity in human tumor cell lines and in animal models of tumor growth.
© 2006 Elsevier Ltd. All rights reserved.

The Src-family of tyrosine kinases, of which Src is the best known, comprises the highly homologous proteins Src, Yes, Fyn, Lyn, Hck, Blk, Brk, Fgr, Frk, Srm, Lck, and Yrk.[1] Gene knockout studies of specific Src-family members have elucidated the roles played in bones, neural development, and myeloid and T cell development and function.[2] Src has been shown to play a role in myocardial infarction,[3] stroke,[4] osteoporosis,[5] neurodegeneration,[6] and is involved in metastases and tumor progression, particularly those of breast, metastatic colorectal,[7] ovarian,[8] and pancreatic cancers.[9–11] Despite evidence of the dysregulation of Src in several cancers, there is no known Src inhibitor approved for solid tumors. Dasatinib, a potent dual inhibitor of Src and Abl, was recently approved for the oral treatment of chronic myelogenous leukemia (CML)[12] and Philadelphia chromosome-positive acute lymphoblastic leukemia (ALL). Currently Dasatinib is in clinical trials for the treatment of solid tumors and gastrointestinal stromal tumors (GIST). On account of the pivotal role played by Src in several oncology and non-oncology disease states, inhibitors of Src have broad potential utility. Several series of Src inhibitors have been reported.[13–20]

We have recently disclosed a novel series of benzotriazine-based compounds as inhibitors of Src.[21] Herein, we describe our continuing efforts in optimizing this benzotriazine series of Src inhibitors, and the identification of an orally active compound with desirable PK properties, activity against selected human tumor cell lines, and demonstrated efficacy in mouse models of tumor growth.

Preliminary SAR studies enabled the identification of key structural requirements of the benzotriazine series

Keywords: Src inhibitor; Cancer; Kinase inhibitor; Benzotriazines.
* Corresponding author. Tel.: +1 858 678 0760; fax: +1 858 678 0762; e-mail: noronha@targegen.com

0960-894X/$ - see front matter © 2006 Elsevier Ltd. All rights reserved.
doi:10.1016/j.bmcl.2006.11.006

that lead to substitutions at the 3-, 5- or 6-, and 7-positions critical for obtaining low nanomolar biochemical potencies.[21] A homology model was constructed for a fully activated Src structure that served to guide compound design and optimization.[22] Figure 1 depicts a minimized binding mode of a benzotriazine inhibitor (**1**) in the ATP pocket of the activated Src model. We have subdivided this ATP-binding pocket of Src into four distinct regions, labeled P1 through P4. The binding interactions of **1** at the ATP pocket are summarized as follows. The 7-substituted phenyl ring binds in the hydrophobic back pocket (the P4 region) positioning this phenyl ring perpendicular to the benzotriazine core. Our earlier studies[21] showed that a limited set of small hydrophobic groups may be substituted on this phenyl ring at very specific positions since the P4 pocket possesses a limited tolerance for larger groups. The 3-aminobenzotriazine moiety forms both donor and acceptor hydrogen bonds to Met-341 in the hinge region (termed P3), thus sharing a common site with the hinge binding purine ring of ATP. The 3-amino group from the benzotriazine core is attached to an aryl linker in a region of the ATP pocket termed P2, which falls in the hydrophobic channel leading out toward a solvent-accessible area. The spacer with a solubilizing group binds in the P1 region of the pocket, an area accessible to solvent. Benzotriazine inhibitors containing a basic nitrogen in the P1 region provide enhanced potency through protonation and interaction with Asp-348.

Motivated by a preliminary optimization of the benzotriazine-based Src inhibitors,[21] we focused our efforts on two compounds. Both possess the 1-ethylpyrrolidinyl moiety, which binds in the P1 region. In the first compound, the 1-ethylpyrrolidinyl group is attached to the 3-aminophenyl ring (P2 region) through an ether linker (**1**), and in the second compound through a sulfonamide linker (**17**). Both linkers place the 1-ethyl pyrrolidine group in the P1 region where the basic nitrogen of the pyrrolidine interacts with Asp-348.

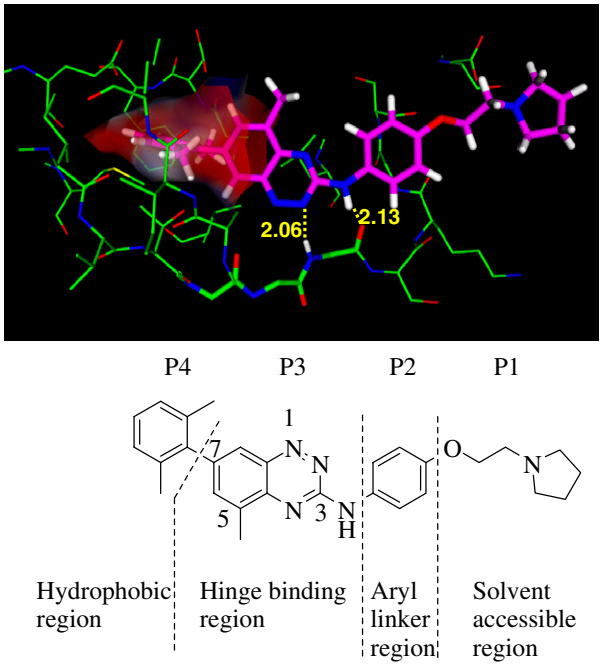

Figure 1. A homology model of the ATP pocket of Src, showing the binding of **1**.

Initial SAR efforts were focused on compounds that have their ethylpyrrolidine moiety in the P1 region, attached to an aryl group (positioned in the P2 region) via an oxygen linker (ether series, Table 1) and exploring various substituents at the 7-position (P4 region) of the benzotriazine ring.[23] The removal of the dimethyl groups on the phenyl ring of **1** results in compound **2** with a 50-fold decrease in potency. The replacement of the dimethyl groups on the 7-phenyl ring in **1** with dichloro resulted in compound **3** with comparable potency. The monochloro analog **4** was three times less potent than the dichloro analog **3**. Compounds with either a 2,6-difluorophenyl substituent at the 7-position (**5**) or a 2-chloro-6-methoxy phenyl at the 7-position (**6**) were 30 times and 70 times less potent than **1**. It appears that fluorine atoms are too small and not as effective as chloro or methyl groups to orinent the phenyl group perpendicular to the benzotriazine ring, a requisite for low nanomolar potency. A methoxy group at the 6-position on the 7-phenyl ring orients the phenyl group perpendicular to the benzotriazine ring, however, the methoxy group may be sterically hindering the binding of the 7-phenyl group within this P4 site (**6**). The binding pocket in the P4 region is tolerant toward small substituents on the 7-phenyl ring, as in the case of methyl groups or chloro groups. The introduction of heteroaromatics in place of the 7-phenyl ring results in decreases in potency as seen with compounds **9**–**12**. The removal of the 5-methyl group on the benzotriazine ring results in a minor loss of potency as seen in compounds **13** and **14**. Both compounds with 5-methyl (**1**) and 6-methyl (**16**) groups on the benzotriazine core share similar potencies.

Table 1. In vitro evaluation of compounds with R^1 and R^2 modifications on the 3-aminobenzo-[1,2,4]-triazine

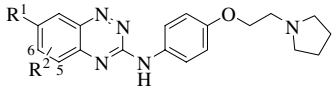

Compound	R^1	R^2	Src (IC_{50} μM)
1	2,6-Me_2 Ph	5-Me	0.007
2	Ph	5-Me	0.341
3	2,6-Cl_2 Ph	5-Me	0.011
4	2-Cl Ph	5-Me	0.035
5	2,6-F_2 Ph	5-Me	0.208
6	2-Cl,6-OMe Ph	5-Me	0.505
7	2-Cl,5-OMe Ph	5-Me	0.778
8	3-Cl,6-OMe Ph	5-Me	1.20
9	4-(2-F, 5-Me pyridyl)	5-Me	0.204
10	4-(3,5-Me_2 isoxazole)	5-Me	0.207
11	4-Pyrimidyl	5-Me	1.5
12	2-Pyridyl	5-Me	1.8
13	2,6-Me_2 Ph	H	0.015
14	2,6-Cl_2 Ph	H	0.030
15	H	H	>10
16	2,6-Me_2 Ph	6-Me	0.012

Table 2. In vitro evaluation of compounds with R^1 and R^2 modifications on the 3-aminobenzo-[1,2,4]-triazine

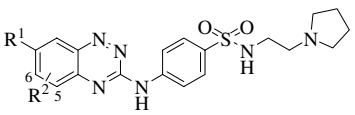

Compound	R^1	R^2	Src (IC_{50} μM)
17	2,6-Me_2 Ph	5-Me	0.009
18	2,6-Cl_2 Ph	5-Me	0.014
19	2-Cl, 6-OH Ph	5-Me	0.013
20	3-CN, 6-Me Ph	5-Me	0.025
21	3-NH_2, 6-Cl Ph	5-Me	0.051
22	3-NH_2	5-Me	0.282
23	3-CH_2NH_2, 6-Me Ph	5-Me	0.353
24	3-NHMe Ph	5-Me	0.631
25	3-$NHSO_2$Me Ph	5-Me	2.90
26	2,6-Me_2 Ph	6-Me	0.011
27	Ph	6-Me	0.315
28	H	6-Me	>10
29	Br	6-Me	>10
30	2-MePh	6-Me	0.01
31	2-CF_3Ph	6-Me	0.067
32	3-CN, 6-Me Ph	6-Me	0.012
33	4-F, 2-Me Ph	6-Me	0.020
34	2-NH_2	6-Me	0.092
35	2-CH_2OH Ph	6-Me	0.072

In parallel, we focused our efforts on optimizing compounds in the sulfonamide series by substituting various groups at the 7-position of benzotriazine ring in P4 region (Table 2). The replacement of the ether linkage in **1** with a sulfonamide group resulted in **17** with comparable potency to **1**. The substitution of dichloro groups on the phenyl ring in place of the dimethyl groups resulted in **18** with comparable potency to **17** and **3**. The replacement of one of the chloro groups with a hydroxy group resulted in **19** without any change in the potency. When one of the *ortho* substituents was moved to *meta* position and substituted with a cyano (**20**) or an amino group (**21**), this resulted in a 3- to 5-fold loss in potency compared to **17**. Moreover, when the *ortho* chloro substituent in **21** was removed as in compound **22**, we saw a 5-fold decrease in potency compared to **21** and a 30-fold drop in potency compared to **17**. These observations are consistent with the SAR from the ether series. It appears that the P4 region accommodates phenyl groups with small substituents at the 2- and the 6-positions. The position of the methyl group (5- or 6-) on the benzotriazine ring did not change the potency as seen with compounds **26** and **17**. The SAR of the 6-methyl series is comparable to that seen in the 5-methyl series. Removal of the bis *ortho* substitutions on the phenyl ring results in compound **27** with a 30-fold loss of potency compared to **17** and **26**. Removal of the 7-phenyl moeity (**28**) or substitution with a bromine (**29**) results in a complete loss of potency. The 2-methylphenyl analog **30** showed comparable potency to **17**, while the 2-trifluoromethyl analog **31** suffered ca. 6-fold loss of potency compared to **30** and **17**. Similarly, the 3-cyano-6-methyl analog **32** shares similar potency to the corresponding 5-methyl analog, **20**. Similar to the 5-methyl benzotriazine analogs, *ortho* substitutions on the 7-phenyl ring in the 6-methyl benzotriazine compounds play an important role in maintaining potency.

It is evident from the above SAR, that the 7-(2,6-dimethyl)phenyl substituted analogs are some of the most potent inhibitors. Therefore, we continued our lead optimization efforts while keeping this 2,6-dimethylphenyl moiety fixed in the P4 region, and exploring various water-soluble groups in the P1 region of the molecule (Table 3).[23] A 2-diethylaminoethoxy group either at the 3-position or at 4-position of the phenyl group in P2 region resulted in **36** and **37**, with comparable potency to **1**. A 2-morpholin-4-ylethoxy group at the 3-position also resulted in a compound (**38**) with comparable potency to **1**. Extending the pyrrolidinyl group in **1** by a methylene unit resulted in compound **39** with comparable potency. Similarly moving the pyrrolidinylethoxy side chain from the 4- to the 3-position on the phenyl

Table 3. In vitro evaluation of compounds with R^4 modifications on the 3-aminobenzo-[1,2,4]-triazine

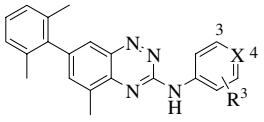

Compound	X	R^3	Src (IC_{50} μM)
36	CH	3-(2-Diethylaminoethoxy)	0.010
37	CH	4-(2-Diethylaminoethoxy)	0.010
38	CH	3-(2-Morpholin-4-ylethoxy)	0.033
39	CH	4-(3-Pyrrolidin-1-yl-propoxy)	0.013
40	CH	3-(2-Pyrrolidin-1-yl-ethoxy)	0.0064
41	CH	4-[2-(4-Methyl-piperazin-1-yl)-ethoxy]	0.021
42	CH	3-[2-(4-Methyl-piperazin-1-yl)-ethoxy]	0.040
43	CH	4-[2-(4-Methyl-piperazin-1-yl)-propoxy]	0.036
44	CH	3-[2-(4-Methyl-piperazin-1-yl)-propoxy]	0.039
45	CH	4-(4′-Methyl-piperazin-1-yl)-amido	0.015
46	CH	4-(Piperazin-1-yl)-amido	0.013
47	CH	4-(*N*-(2-Pyrrolidin-1-yl-ethyl)-benzamide)	0.016
48	CH	3-(*N*-(2-Pyrrolidin-1-yl-ethyl)-benzamide)	0.018
49	N	3-(2-Pyrrolidin-1-yl-ethoxy)	0.0064

group in the P2 region resulted in compound **40** with comparable potency. The 4-methylpiperazinyl group with an ethoxy linker at the 4-position (**41**) or at the 3-position (**42**) resulted in compounds with comparable potencies. The linker in compounds **41** and **42** was extended by one more methylene group to give compounds **43** and **44**, respectively, with no change in enzymatic activity. The oxygen linkers in compounds **1** and **40** were substituted with amide linkers resulting in compounds **47** and **48**, once again with comparable activity. Substitution of the phenyl group in the P2 region with a pyridyl ring resulted in **49** with equally good potency. It appears that the P1 region is tolerant toward a wide number of water-soluble groups.

Modeling studies of the benzotriazine inhibitors suggest that the 5- and 6-positions of the benzotriazine ring in the P3 region are oriented toward the sugar binding pocket and away from the hinge region, and potentially this portion of the inhibitors might be tuned to take advantage of potential binding interactions and to provide for property diversification. A limited number of hydrophilic groups were substituted in place of the 5-methyl group in order to explore this space in the enzyme. Substitution of the 5-methyl group with an amino (**50**), an, methylamino (**51**), an acetamido (**52**), or a methylsulfonamido (**53**) moiety all resulted in compounds with comparable potency to **1** (Table 4).

Table 4. In vitro evaluation of compounds with R^2 modifications on the 3-aminobenzo-[1,2,4]-triazine

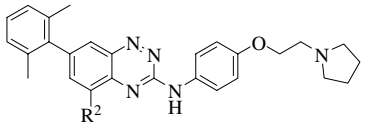

Compound	R^2	Src (IC_{50} μM)
50	NH_2	0.010
51	NHMe	0.010
52	$NHCOCH_3$	0.014
53	$NHSO_2Me$	0.021

The benzotriazines studied were synthesized as shown in Scheme 1. Appropriately substituted 3-bromo-2-nitroanilines (**54**) were reacted with cyanamide under acidic conditions to give intermediate guanidines, which were cyclized with sodium hydroxide to give 1-oxobenzotriazines (**55**).[24,25] These *N*-oxides (**55**) were reduced using Raney nickel to give 3-amino-7-bromobenzotriazines in good yield. Various aryl-substituted benzotriazines (**56**) were prepared by treating 3-amino-7-bromobenzotriazines with aryl boronic acids under Suzuki coupling conditions.[26] The final compounds (**1**–**49**) were prepared from **56** in good yield by using palladium- and xantphos-catalyzed amination.[27] The synthesis of **50**–**53** started with **57**, which was prepared from **54**, as described above. The nitration of **57** resulted in **58** with exclusive nitration at 5-position in good yield. Oxobenzotriazines **58** were subjected to Suzuki and palladium-catalyzed amination couplings as described above followed by the reduction of the nitro group to amine (**60**) using 10% Pd on carbon under hydrogen atmosphere. The amine group in **60** was functionalized with appropriate alkyl halides or acid chlorides to give **50**–**53** in good yield.

Several of these potent compounds shown in Tables 1–3 were tested in a murine CT-26 carcinoma cell assay for further evaluation.[28] Based on the potency in the cell and the biochemical assays, eight compounds (with IC_{50} less than 10 μM in the cell assay) were selected for additional profiling. The cell data for these eight compounds are collected beneath the graph in Figure 2.

The selected compounds were then evaluated in a pulmonary metastases model.[29,30] Control mice treated with vehicle showed extensive tumor burden in the lung (Fig. 2). Compounds were administered to mice (50 mg/kg, i.p., q3d) and all the compounds showed reduction in tumor volume compared to vehicle control.[31] The greatest reduction in tumor volume (60%) compared to vehicle control was seen with compound **3**. Compounds **1**, **45**, and **49** showed equal reduction in tumor burden.

Based on the above initial screening, compounds **1** and **3** were selected for protein binding assays and pharmaco-

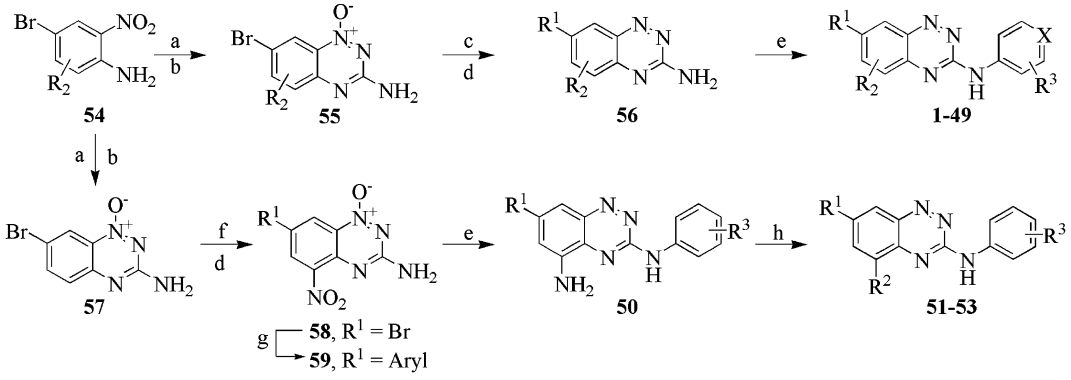

Scheme 1. Reagents and conditions: (a) NH_2CN, 37% aq HCl, 110 °C, 1.5 h; (b) 30% aq NaOH, 110 °C, 0.5 h, 65% over two steps; (c) 10% Raney Ni, H_2, EtOH, 22 °C, 4 h, 70–80%; (d) $R^1B(OH)_2$, $Pd(PPh_3)_4$, K_2CO_3, DME/EtOH/H_2O (4:1:1), Δ, 3 h, 80%; (e) R^3Ar or HetArBr, $Pd_2(dba)_3$, xantphos, Cs_2CO_3, dioxane, Δ, 12 h, 50–70%; (f) H_2SO_4/HNO_3 (1:1), 22 °C, 16 h, 95%; (g) H_2, 10% Pd/C, EtOH, 22 °C, 12 h, 70–80%; (h) R^2Cl, CH_2Cl_2, 22 °C, 1 h, 70–80%.

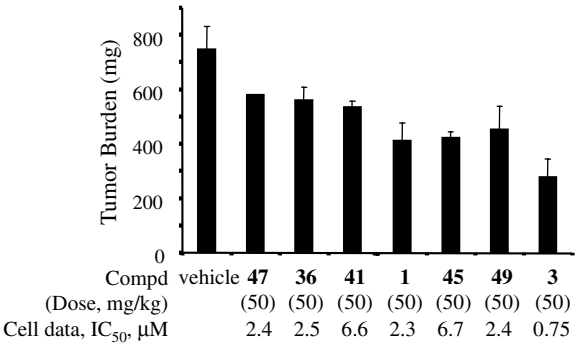

Figure 2. Tumor burden model with murine CT-26 carcinoma cells. Compounds were dosed ip, q3d. The IC_{50} values for these compounds in murine CT-26 carcinoma cell line are shown.

kinetic (PK) studies (Table 5). Both compounds showed high protein binding to human plasma.[32] We examined the PK properties of compounds **1** and **3** in mouse, rat, and dog. Both compounds showed C_{max} between 300 and 1000 ng/mL (ca. 0.6–2 μM) in all three species with the exception of compound **1** in the dog where the C_{max} was 5240 ng/mL (>10 μM). Both compounds have favorable bioavailability (74–86%) in mouse plasma after oral dosing. Compounds **1** and **3** showed comparable PK data in rat and differ significantly in dog. These compounds have very long $T_{1/2}$ in dog, followed by mouse and moderate $T_{1/2}$ in rat. The clearance and volume of distribution of **3** in dog were much higher than those shown by **1**. Both compounds were evaluated for their Cyp inhibition profile and found to be very weak inhibitors of various Cyp isozymes (Table 6). Based on the PK parameters and activity in the above screening tumor model, compound **3** was selected for further characterization.

Table 6. In vitro evaluation of three compounds in various CYP isozymes

Compound	CYP isozymes (IC_{50}, μM)				
	3A4	1A2	2C9	2C19	2D6
1	42	>100	>100	12	25
3	62	>100	>100	12	33

Compound **3** was evaluated in an A549 human NSCLC xenograft model (Fig. 3),[33] along with Tarceva[34] as positive control.[35] At 25 mg/kg, i.p., qod, compound **3** showed potency comparable to Tarceva at 80 mg/kg, po, qod. Moreover, at the higher dose of 40 mg/kg, compound **3** showed 86% reduction in tumor burden compared to the vehicle control. In order to establish a link between the molecular target of **3** and its pharmacodynamic effects, the impact of **3** on Src kinase activities was examined in tumor tissue in vivo.[36] The Tyr-861 residue of Focal Adhesion Kinase (Fak) is a specific substrate for Src.[37–39] Compound **3** inhibited phosphorylation of Fak-Y861 in these tumors in a dose-dependent manner, with full inhibition at 40 mg/kg (Fig. 3), suggesting that compound **3** was inhibiting Src in vivo.[40] This in vivo inhibition of the phosphorylation of Fak-Y861 in a dose-dependent manner suggests that Fak-Y861 has potential utility as a biomarker of compound activity in clinical biopsy samples.

Compound **3** was evaluated in a selected panel of kinases (Table 7) and in general showed a low level of selectivity against closely related Src family members, other structurally related intracellular kinases, and a moderate level of selectivity versus selected serine threonine and certain receptor kinases. Compound **3** was also evaluated in a select panel of cell-based assays for its

Table 5. In vitro evaluation in protein binding assay, and in vivo PK parameters (25 mg/kg, po)

Compound	Protein binding human plasma	Species	C_{max} (ng/mL)	T_{max} (h)	$T_{1/2}$ (h)	AUC (h ng/mL)	CL_{sys} (mL/min/kg)	V_{dss} (L/kg)	F (%)
1	>99.9%	Mouse	790	6	9.5	19,070	18.8	11.4	86
1		Rat	419	6	5.6	9570	9.2	7.2	20
1		Dog	5240	1.5	19	9680	5.1	8.6	68
3	99.8%	Mouse	415	8	8	15,300	12.7	16.1	74
3		Rat	348	8.8	4.6	8010	12.7	9.4	35
3		Dog	679	4	13	8680	14.5	18.7	42

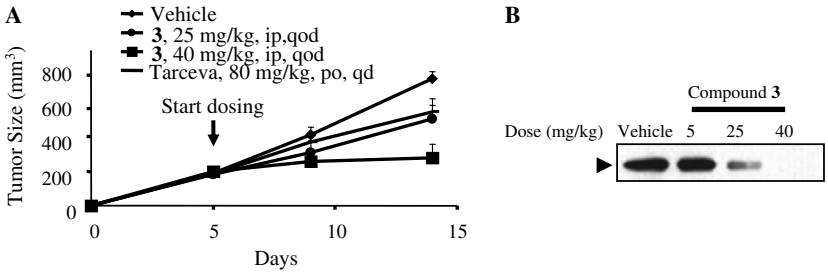

Figure 3. (A) Compound **3** inhibited the growth of A549 human NSCLC xenografts. The compound was administered ip starting on day 5. (B) Proteins from the tumors were examined by immunoblotting using a polyclonal antibody directed against phospho-Focal Adhesion Kinase (Fak)-Y861.

Table 7. In vitro evaluation of **3** in a selected panel of kinases

Kinase	K_i (nM)	Kinase	K_i (nM)
Src	28.1 ± 2.1	VEGF-R2	784 ± 96
Yes	12.9 ± 1.9	FGF-R1	493 ± 102
Lck	29.4 ± 3.4	PDGFRβ	2090 ± 670
Lyn	25.9 ± 1.2	EphB4	63.8 ± 5.2
Abl	19.4 ± 3.5	Ret	407 ± 109

Table 8. In vitro evaluation of **3** in selected tumor cell lines

Cell line	Tumor type	IC_{50} μM
Molt-4	Leukemia	0.250
K562	Leukemia	0.215
CT-26	Colon	0.750
Colo-205	Colon	2.50
HT-29	Colon	>5.00
MDA-MB231	Breast	0.240
MCF-7	Breast	0.085
A549	NSCLC	0.900

selectivity (Table 8). The potency of compound **3** was less than 1 μM in all the cell lines tested except Colo-205 (IC_{50} = 2.5 μM) and HT-29 (IC_{50} > 5.0 μM).

In summary, this work describes efforts that led to an increased understanding of the binding of these benzotriazines in the ATP pocket of Src, and resulted in marked improvements in potency, and improved PK properties. Further, lead optimization efforts unveiled the activity of **3** against selected human tumor cell lines, and demonstrated efficacy of **3** in mouse xenograft models driven by Src mediated pathways. Compound **3** has potential use in the treatment of cancers of the colon, liver, pancreas, breast, brain, and bladder, where Src activity is dysregulated.[41] Detailed studies on systemic PK, metabolism, tolerability, and toxicity of compound **3** were completed and will be disclosed separately.

References and notes

1. Trevino, J. G.; Summy, J. M.; Gallick, G. E. *Mini Rev. Med. Chem.* **2006**, *6*, 109.
2. Lowell, C. A.; Soriano, P. *Genes Dev.* **1996**, *10*, 1845.
3. Weis, S.; Shintani, S.; Weber, A.; Kirchmair, R.; Wood, M.; Cravens, A.; McSharry, H.; Iwakura, A.; Yoon, Y.; Himes, N.; Burstein, D.; Doukas, J.; Soll, R.; Losordo, D.; Cheresh, D. *J. Clin. Invest.* **2004**, *113*, 885.
4. Paul, R.; Zhang, Z. G.; Eliceiri, B. P.; Jiang, Q.; Boccia, A. D.; Zhang, R. L.; Chopp, M.; Cheresh, D. A. *Nat. Med.* **2001**, *7*, 222.
5. Susva, M.; Missbach, M.; Green, J. *Trends Pharmacol. Sci.* **2000**, *21*, 489.
6. Yeatman, T. J. *Nat. Rev.* **2004**, *4*, 470.
7. Talamonti, M. S.; Roh, M. S.; Curley, S. A.; Gallick, G. E. *J. Clin. Invest.* **1993**, *91*, 53.
8. Wiener, J. R.; Windham, T. C.; Estrella, V. C.; Parikh, N. U.; Thall, P. F.; Deavers, M. T.; Bast, R. C.; Mills, G. B.; Gallick, G. E. *Gynecol. Oncol.* **2003**, *88*, 73.
9. Ito, H.; Gardner-Thorpe, J.; Zinner, M. J.; Ashley, S. W.; Whang, E. E. *Surgery* **2003**, *134*, 221.
10. Summay, J. M.; Gallick, G. E. *Cancer Metastasis* **2003**, *22*, 337.
11. Irby, R. B.; Yeatman, T. J. *Oncogene* **2000**, *19*, 5636.
12. Kanerva, J.; Nwawka, O.; Hwang1, K.; Lee, F. Y.; Corey, S. J. *Blood* **2004**, *104*, Abstract 4480.
13. Boschelli, D. H.; Wu, B.; Sosa, A. C. B.; Durutlic, H.; Ye, F.; Raifeld, Y.; Golas, J. M.; Boschelli, F. *J. Med. Chem.* **2004**, *47*, 6666.
14. Boschelli, D. H.; Wu, B.; Sosa, A. C. B.; Durutlic, H.; Chen, J. J.; Wang, Y.; Golas, J. M.; Lucas, J.; Boschelli, F. *J. Med. Chem.* **2005**, *48*, 3891.
15. Boschelli, D. H.; Wu, B.; Sosa, A. C. B.; Chen, J. J.; Golas, J. M.; Boschelli, F. *Bioorg. Med. Chem. Lett.* **2005**, *15*, 4681.
16. Manetti, F.; Locatelli, G. A.; Maga, G.; Schenone, S.; Modugno, M.; Forli, S.; Corelli, F.; Botta, M. *J. Med. Chem.* **2006**, *49*, 3278.
17. Carraro, F.; Naldini, A.; Pucci, A.; Locatelli, G. A.; Maga, G.; Schenone, S.; Bruno, O.; Ranise, A.; Bondavalli, F.; Brullo, C.; Fossa, P.; Menozzi, G.; Mosti, L.; Modugno, M.; Tintori, C.; Manetti, F.; Botta, M. *J. Med. Chem.* **2006**, *49*, 1549.
18. Dalgarno, D.; Stehle, T.; Narula, S.; Schelling, P.; van Schravendijk, M.; Adams, S.; Andrade, L.; Keats, J.; Ram, M.; Jin, L.; Grossman, T.; MacNeil, I.; Metcalf, C.; Shakespeare, W.; Wang, Y.; Keenan, T.; Sundaramoorthi, R.; Bohacek, R.; Weigele, M.; Sawyer, T. *Chem. Biol. Drug Des.* **2006**, *67*, 46.
19. Wang, Y.; Metcalf, C.; Shakespeare, W.; Sundaramoorthi, R.; Keenan, T.; Bohacek, R.; Van Schravendijk, M.; Violette, S.; Narula, S.; Dalgarno, D.; Haraldson, C.; Keats, J.; Liou, S.; Mani, U.; Pradeepan, S.; Ram, M.; Adams, S.; Weigele, M.; Sawyer, T. *Bioorg. Med. Chem. Lett.* **2003**, *13*, 3067.
20. Honold, K.; Kaluza, K.; Masjost, B.; Schaefer, W.; Scheiblich, S. Hoffmann-La Roche, WO2006066913, 2006.
21. Noronha, G.; Barrett, K.; Cao, J.; Dneprovskaia, E.; Fine, R.; Gong, X.; Gritzen, C.; Hood, J.; Kang, X.; Klebansky, B.; Lohse, D.; Mak, C. C.; McPherson, A.; Palanki, M. S. S.; Pathak, V. P.; Renick, J.; Soll, R.; Splittgerber, U.; Wrasidlo, W.; Zeng, B.; Zhao, N. *Bioorg. Med. Chem. Lett.* **2006**, *16*, 5546.
22. The fully activated catalytic domain of human Src kinase was built based on available crystal structures of activated Lck. The catalytic domains of Src and Lck exhibit 67% sequence identity over 273 residues without gaps in the alignment with significantly higher homology exhibited in the ATP-binding site. The model was built using the interactive programs InsightII and Homology from Accelrys. Ligands were docked initially into the active site *using* an automated modeling program BioDock (NIH SBIR Grant 1R43GM071055) and subsequently using interactive modeling in InsightII. Models with and without ligands were subjected to energetic refinement including solvent using the Accelerys program Discover. Visualization was generated using the program BioInterpreter (NIH SBIR Grant 5R44GM061465).
23. A portion of the material presented in this paper was disclosed in two posters. (a) McPherson, A.; Barrett, K.; Cao, J.; Gritzen, C.; Hood, J.; Mak, C. C.; Noronha, G.; Pathak, V. P.; Renick, J.; Soll, R.; Splittgerber, U.; Zeng, B. *Abstracts of Papers*, 231st National Meeting of the American Chemical Society, Atlanta, GA, March 26–30, 2006; American Chemical Society: Washington, DC, 2006; (b) Mak, C. C.; Barrett, K.; Cao, J.; Gritzen, C.; Hood, J.; McPherson, A.: Noronha, G.; Pathak, V. P.; Renick, J.; Soll, R.; Splittgerber, U.; Zeng, B. *Abstracts of Papers*, 231st National Meeting of the American Chemical Society, Atlanta, GA, March 26–30, 2006; American Chemical Society: Washington, DC, 2006; MEDI-065.
24. Arndt, F. *Ber.* **1913**, *46*, 3522.
25. Mason, J. C.; Tennant, G. *J. Chem. Soc. (B)* **1970**, 911.

26. Kudo, N.; Perseghini, M.; Fu, G. C. *Angew. Chem., Int. Ed.* **2006**, *45*, 1282.
27. Tundel, R. E.; Anderson, K. W.; Buchwald, S. L. *J. Org. Chem.* **2006**, *71*, 430.
28. Approximately 3000 CT-26 cells were added to 96-well plates suspended in RPMI 1640 medium containing 10% FBS, penicillin, streptomycin, and glutamine. Compounds, dissolved in DMSO and ranging in concentration from 5 to 10,000 nM, were added to a total of 1% of the total assay volume. After these assays were incubated in a 10% carbon dioxide environment for 72 h at 37 C, XTT was added and allowed to proceed for an additional 4 h. Remaining cellular activity was assessed by reading the absorbance at 492. After subtracting background absorbance at 650 nm, data analysis was done by using the nonlinear graphing capabilities of GraphPad PRIZM, Ver. 4.01.
29. Hood, J. D.; Bednarski, M.; Frausto, R.; Guccione, S.; Reisfeld, R. A.; Xiang, R.; Cheresh, D. A. *Science* **2002**, *296*, 2404.
30. In order to establish pulmonary metastases model, murine CT-26 carcinoma cells were injected intravenously into BALB/c mice. This typically results in the formation of lung metastases within four days. In this study, establishment of pulmonary metastases was extended to 10 days before treatment with the compounds to ensure that all animals contained actively growing lung tumors.
31. The frequency and the amount of doses for this study were chosen based on the preliminary PK studies on these compounds (data not shown). These are not minimum tolerated doses.
32. Eriksson, M. A. L.; Gabrielsson, J.; Nilsson, L. B. *J. Pharm. Biomed. Anal.* **2005**, *38*, 381.
33. A549 tumors were formed by implanting 1×10^6 cells subcutaneously on the flanks of immunocompromised (nu/nu) mice ($n = 6$). When the tumors reached 100 mm^3, compounds were administered ip in a solution of Solutol:PEG:EtOH:Water = 10:10:10:70 formulation on day 5 using every other day (QOD) dosing schedule. Tumor volumes were calculated using caliper measurements and the ellipsoid formula. The experiment was ended when vehicle-treated tumors showed signs of necrosis.
34. Ji, H.; Zhao, X.; Yuza, Y.; Shimamura, T.; Li, D.; Protopopov, A.; Jung, B. L.; McNamara, K.; Xia, H.; Glatt, K. A.; Thomas, R. K.; Sasaki, H.; Horner, J. W.; Eck, M.; Mitchell, A.; Sun, Y.; Al-Hashem, R.; Bronson, R. T.; Rabindran, S. K.; Discafani, C. M.; Maher, E.; Shapiro, G. I.; Meyerson, M.; Wong, K. *Proc. Natl. Acad. Sci. U.S.A.* **2006**, *103*, 7817.
35. Currently Tarceva is recommended as a monotherapy for the treatment of patients with locally advanced or metastatic non-small cell lung cancer (NSCLC) after failure of at least one prior chemotherapy regimen. Tarceva is an approved agent for treating NSCLC. Therefore, it is important to test the new compounds for treating NSCLC against the approved and established therapeutic agent, Tarceva.
36. Colon tumor xenografts were formed by injecting 10^6 Colo-205 cells subcutaneously on the flank of nude mice (nu/nu) ($n = 5$). By day 5, mean tumor size (as measured using hand calipers) was 100–150 mm^3 using the ellipsoid formula. At this point animals were randomized so that all groups had approximately the same mean tumor volume and compound was administered at via oral gavage in a Phosal 50 PG formulation.
37. Calalb, M.; Zhang, X.; Polte, T.; Hanks, S. *Biochem. Biophys. Res. Commun.* **1996**, *228*, 662.
38. Lim, Y.; Han, I.; Jeon, J.; Park, H.; Bahk, Y.; Oh, E. *J. Biol. Chem.* **2004**, *279*, 29060.
39. Eliceiri, B.; Paul, R.; Schwartzberg, P.; Hood, J. D.; Leng, J.; Cheresh, D. *Mol. Cell* **1999**, *4*, 915.
40. Colo-205 tumors were subcutaneously implanted in mice and allowed to grow to 100–150 mm^3. Six hours after the compound **3** was administered orally, tumors were resected from the animals for Western blot analysis using a polyclonal antibody directed against Fak-Y861.
41. Tsygankov, A. Y.; Shore, S. K. *Curr. Pharm. Des.* **2004**, *10*, 1745.